energies

MDPI

Article

PMSM Field-Oriented Control with Independent Speed and Flux Controllers for Continuous Operation under Open-Circuit Fault at Light Load Conditions

Haneen Ghanayem *, Mohammad Alathamneh and R. M. Nelms

Electrical and Computer Engineering Department, Auburn University, Auburn, AL 36849, USA; mqa0002@auburn.edu (M.A.); nelmsrm@auburn.edu (R.M.N).
* Correspondence: hig0002@auburn.edu

Abstract: Presented in this article is a permanent magnet synchronous motor (PMSM) control under open-circuit fault (OCF) operation using field-oriented control (FOC) with independent speed and flux controllers. The independent control allows the motor to operate efficiently under varying conditions. A simplified control approach is employed to control the PMSM under the OCF situation; the actual flux and torque of the PMSM are directly measured by the stator currents, eliminating the need for estimators or phase-locked-loop (PLL) systems. Matlab/Simulink is employed for the simulation, while hardware experiments are conducted using a dSPACE DS1104. The simulation and the hardware results demonstrate the control method's effectiveness in maintaining continuous motor operation during OCF, its robustness against OCF conditions, and its ability to adapt under varying conditions, including speed, flux, and load torque change.

Keywords: field-oriented control; three-phase PMSM; open-circuit fault; flux controller; decoupled control

Citation: Ghanayem, H.; Alathamneh, M.; Nelms, R.M. PMSM Field-Oriented Control with Independent Speed and Flux Controllers for Continuous Operation under Open-Circuit Fault at Light Load Conditions. *Energies* **2024**, *17*, 593. https://doi.org/10.3390/en17030593

Academic Editor: Muhammad Ammirrul Atiqi Mohd Zainuri

Received: 28 November 2023
Revised: 23 January 2024
Accepted: 24 January 2024
Published: 26 January 2024

1. Introduction

Permanent magnet synchronous motors (PMSMs) are extensively used in various industrial applications because of their compact design, lightweight nature, capacity to deliver precise control, high efficiency, and excellent dynamic characteristics [1]. Different control methods are employed to regulate the speed of the PMSM. The control method can be either a scalar control or a vector control. Figure 1 illustrates the various control method classifications of a PMSM [2]. Among them, the field-oriented control (FOC) technique is considered the most popular technique in PMSM control.

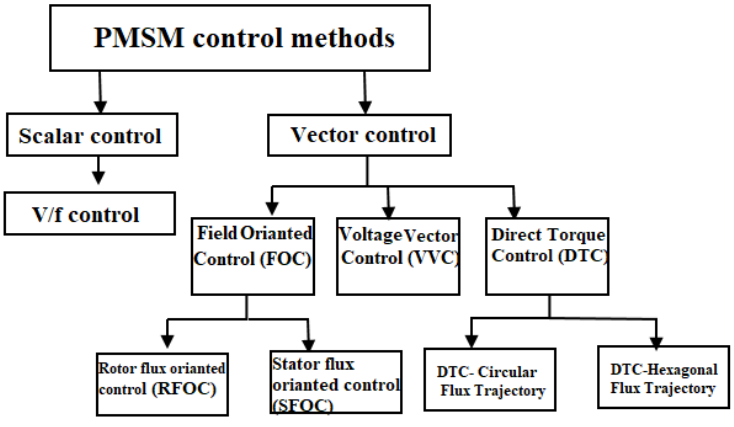

Figure 1. PMSM control techniques.

Presented in [3,4] is a comparative performance of PMSM based on FOC and direct torque control (DTC) methods. The motor position was determined by a mechanical sensor while the flux and the torque estimators were designed to achieve the DTC technique. In addition, the performance of the PMSM using DTC scheme based on space vector pulse width modulation (SVPWM) method was discussed in [5]. Proposed in [6] is a PMSM control based on model predictive current controller (MPC). The speed response was evaluated based on the MPC and the traditional control method. The comparative analysis of simulation and experimental outcomes indicated that, based on MPC, the motor has a fast speed response and small steady-state errors under the rated load. Proposed in [7] is a model predictive speed control of PMSM. The proposed method improved the overall motor performance. Proposed in [8] is the embedded system implementation of a senseless PMSM control based on FOC strategy. The proposed control method was used to identify the mechanical and electrical parameters of PMSM.

In recent years, faults have become a popular issue that may occur with motors. PMSM may experience different types of faults, such as electrical, mechanical, and magnetic faults [9]. The OCF is considered the most common electrical fault type and will be presented in this article. It leads to significant changes in motor performance; it may cause large torque ripples and serious mechanical vibration and stress. Hence, a special control strategy is required to maintain speed control [10]. The study in [11] presented a control method for a PMSM that achieves separate speed and flux control without the need for estimators, demonstrating its effectiveness through simulations and experimental results.

In general, fault diagnosis involves the process of identifying and localizing the OCF of PMSM. This process aims to ensure the early detection of faults, prevent system breakdowns, and minimize maintenance costs. Fault diagnosing methods for Brushless DC motors (BLDC) was presented in [12].The proposed control method eliminates the need for additional voltage sensors, has fast fault detection, and has a high level of robustness in the control system. Proposed in [13] is an open-circuit fault diagnosis method for the three-phase inverter connected to brushless motor. The simulation outcomes provide that the suggested method can effectively detect and localize OCF involving a single switch, dual switches, three switches, and even a four-switch fault.

Discussed in [14] is an open-circuit fault tolerance control of dual three-phase PMSM. The torque superposition compensation control (TSC) was proposed to increase the capability of torque production and reduce copper losses. The simulation outcomes validated the efficiency of the suggested TSC fault-tolerant control strategy. Presented in [15] is an open-circuit fault diagnosis method of PMSM based on the model predictive current control (MPCC) technique. The experimental results validated the accuracy of the diagnostic algorithm in detecting and locating single and multiple OCFs. A symmetrical and DC component diagnosis method for a PMSM drive for single and two OCFs conditions was discussed in [16].

Proposed in [17] is fault tolerance control (FTC) for a five-phase PMSM under open-circuit fault conditions. FTC was employed to mitigate the effects of an open phase. The proposed control method has a significant improvement in torque and speed ripples during OCF operation. In [15], the authors proposed a model predictive current control (MPCC) and cost function error for PMSM operation under an OCF. The proposed control method was able to detect the fault type and its location. Furthermore, it has strong robustness against parameter variation. An evaluation was conducted in [18] to compare the fault tolerance control of a five-phase PMSM using model predictive current control (MPCC) and model predictive torque control (MPTC) during open-circuit fault operation. The performance of the two methods under OCF operation was included. Discussed in [19] is the operation of a five-phase PMSM under open-circuit fault conditions utilizing model predictive torque control and space vector modulation (MPTC-SVM). Using MPTC-SVM provides a good transient response, improves the overall performance, and reduces the harmonics. Proposed in [20] is a fault tolerance control of a six-phase asymmetric PMSM under OCF operation. Space-vector modulation using direct-torque control (SVM-DTC)

was used. By implementing the suggested control method, the variation in torque was minimized to a range of ±2%. The study in [21] proposes a model-based current-signature algorithm for diagnosing power switch faults in three-phase PMSM. The algorithm utilizes online ellipse fitting to reconstruct current phasor trajectories, successfully detecting and isolating open circuits in power switch converters with minimal latency, demonstrating robustness against transient dynamics. A three-stage hybrid fault diagnosis approach for open-circuit faults in Insulated—Gate Bipolar Transistors (IGBTs) within Voltage Source Inverter (VSI)-fed PMSM drive systems for Hybrid Electric Vehicles (HEVs) was proposed in [22]. The method combines model-based FOC with a data-driven approach using the Modified Multi-Class Support Vector Machine (MMC-SVM) algorithm to detect, locate, and clear IGBT faults without additional sensors. The approach shows robustness against various fault scenarios, ensuring continuous operation and recovery of the electric drive-motor system.

A predictive current control-based fault-tolerant scheme for PMSM drives was proposed in [23], addressing open-phase and open-switch faults without auxiliary circuits. The scheme optimizes fault-tolerant performance, considering torque ripple and copper loss. For open-phase faults, fault-tolerant current references are derived, then optimized to reduce copper loss without increasing torque ripple. For open-switch faults, a two-mode current control is designed to utilize the remaining healthy switch, reducing copper loss and torque ripple. Reference [24] proposes a fast diagnosis strategy for open-circuit faults in switch devices within the dual inverter topology of an open-winding PMSM system. The strategy, based on voltage error estimation, analyzes the inverter output characteristics before and after faults. The method eliminates the need for additional voltage sensors reduces diagnosis time, and is insensitive to PWM strategy nuances.

Diagnosing multiple open-circuit faults in IGBTs in electric vehicles using three-phase currents without relying on motor models or control parameters was studied in [25]. A vector-controlled PMSM drive with a PR controller under OCF was proposed in [26], utilizing FOC with PWM technology.

The paper in [27] addresses the challenge of high torque ripple in PMSMs, which negatively impacts motor performance, reliability, and efficiency. The proposed adaptive PIR current controller, integrating a resonant controller, exhibits superior performance, achieving a notable 21% reduction in torque ripple compared to conventional PI control methods, as validated through hardware experiments.

Proposed in [28] are two model predictive controllers for three-phase Surface-mounted PMSM considering an open-circuit fault, which are used for pre-fault and post-fault operations. Presented in [29] is an open-circuit fault of a dual three-phase PMSM based on sensorless DTC and a modified flux observer. The flux observer is used to obtain DTC, while the position is detected using a normalized phase-locked loop (PLL). Thus, the proposed method improved the torque response without a position sensor. Three-phase fault tolerance control of PMSM under open-circuit fault based on deadbeat-direct torque and flux control (DB-DTFC) was investigated in [30]. In [31], five-phase fault-tolerant PMSM based on the Remedial Field-Oriented Control (RFOC) method was studied under open-circuit fault conditions. Presented in [32] is a fault tolerance control of modular motors under open-circuit fault, which is also known as extended open-circuit fault-tolerant control (EOCFTC). Based on the EOCFTC's proposed control method, the motor operated steadily and reliably under the OCF with constant output torque. In [33], a five-phase integrated modular PMSM with an optimal fault-tolerance control method under open-circuit fault conditions was studied. The implemented control strategy guaranteed stable motor operation in the presence of open-circuit fault, effectively minimizing any torque fluctuations. Presented in [34] is direct torque control of a five-phase PMSM based on a virtual stator flux strategy under open-circuit fault operation. This control strategy smoothed out the torque response and provided high dynamic performance.

The research in [35] introduces a voltage residual analysis method for diagnosing an inverter open-circuit fault without extra sensors, relying on DC and second harmonic

components for fast and reliable detection. The proposed technique, verified through simulations and testing, proves effective and robust for fault diagnosis in various operating conditions. Reference [36] reviews open-winding PMSMs (OW-PMSMs), emphasizing their potential as fault-tolerant direct-drive generators in wind energy conversion systems. The common DC bus configuration is identified as promising for fault tolerance, yet the presence of a zero-sequence current poses a challenge, prompting the need for control algorithms to address this issue. The study identifies literature gaps in existing control techniques, hindering comprehensive extensions for OW-PMSMs in fault-tolerant wind energy systems. The study in [37] introduces a novel fault-tolerant control strategy for PMSMs, proposing a natural full range minimum-loss approach based on analyzing current relations. Unlike traditional methods, it avoids complex fault diagnosis and optimization processes, demonstrating smooth pre-fault to post-fault transition and improved operational performance in experiments.

In general, under the open-circuit fault, the balanced system of the PMSM is disrupted, causing serious effects on motor performance. Hence, different control strategies are required to enhance the motor's operation under the open-circuit fault. Fault tolerance control, model predictive control, and senseless control methods can all be used during the open-circuit fault. Thus, some of these methods may require adaptive estimators, which can estimate the faulted-phase current, speed, or angular position, to predict the response and maintain the motor's performance. Nevertheless, in this article, the motor is controlled during open-circuit fault operation by employing separate controllers for speed and flux, ensuring independence between them. The flux and torque feedback signals are obtained directly from the stator currents, eliminating the requirement for designing flux/torque estimators.

This paper investigates the performance of a three-phase PMSM under open-circuit fault conditions. The study utilizes decoupled speed and flux control methods to enable independent operation. By incorporating separate flux control, traditional field-oriented control techniques are adapted, eliminating the need for a dedicated flux or torque observer. The research assesses the PMSM's performance under different scenarios, such as speed, flux, and load torque variations during the open-circuit fault condition. The suggested control method ensures continuous and stable motor operation, highlighting its reliability and dynamic performance effectively.

The unique contributions of this study are outlined below:

- Enhance the reliability of the drive system and ensure continuous motor operation in the presence of open-circuit faults.
- Achieve resilient control capable of managing variations in flux, speed, and load under open-circuit fault conditions.
- Achieve separate control over flux and speed in the presence of open-circuit faults.
- Apply a direct control method that eliminates the need for speed/position estimators and flux/torque observers.

This paper is organized as follows: Section 1 presents the introduction and an overview of the subject matter. Section 2 outlines the modeling methodology for a three-phase permanent magnet synchronous motor (PMSM) experiencing an open-circuit fault (OCF). The control algorithm and strategy are described in Section 3. The simulation results are presented in Section 4, while Section 5 showcases the experimental findings. Lastly, Section 6 offers a concise summary and conclusion of this article.

2. Modeling Approach of Three-Phase PMSM Drive under Open-Circuit Fault

The mathematical model of a PMSM can be presented in dq-coordinate. Equations (1) and (2) represent the stator voltages of the motor. Similarly, Equations (3) and (4) depict the stator flux equations in the dq-coordinate system. The torque expression is shown in Equation (5).

$$V_d = R_s I_d + L_d \frac{dI_d}{dt} - \omega_s \psi_q \tag{1}$$

$$V_q = R_s I_q + L_q \frac{dI_q}{dt} - \omega_s \psi_d \tag{2}$$

$$\psi_d = L_d I_d + \psi_m \tag{3}$$

$$\psi_q = L_q I_q \tag{4}$$

$$T_e = \frac{3}{2} p(\psi_d I_q - \psi_q I_d) \tag{5}$$

For surface-mounted PMSM (SPMSM), $L_d = L_q = L_s$, the torque equation can be rearranged to be as shown in Equation (6).

$$T_e = \frac{3}{2} p(\psi_m I_q) = K_t I_q \tag{6}$$

As shown in Equations (3) and (5), the stator flux and the torque can be controlled independently by the currents I_d and I_q, respectively. Thus, decoupled control of torque and flux can be achieved.

Under open-circuit fault operation, the balanced current of the motor system is disrupted, causing an imbalance between the remaining two phases. The current through the open phase will drop to zero. However, the amplitude of the two other phases will be increased by $\sqrt{3}$. The stator currents during the OCF are as follows [38]:

$$\begin{cases} i_a = 0 \\ i_b = \sqrt{3} I_m [sin(\theta - \frac{2\pi}{3}) + \frac{1}{2} sin(\theta)] \\ i_c = \sqrt{3} I_m [sin(\theta + \frac{2\pi}{3}) + \frac{1}{2} sin(\theta)] \end{cases} \tag{7}$$

3. Control Algorithm of OCF-Decoupled Speed and Flux Controllers

The utilization of FOC, incorporating independent speed and flux controllers, ensures the continuous operation of the motor during the OCF condition. The PI-flux controller is proposed to compensate for the open-circuit fault and generate i_d^*. The speed controller is utilized to produce the torque reference and i_q^* value, aiming to achieve optimal performance. Then, the dq-axis reference voltages are generated by the current controllers. The current controllers are implemented using the PI control method. As a result, two different controllers are utilized to regulate the speed and flux, utilizing two PI current controllers to regulate the dq- currents. The d-axis reference current is generated through the flux controller. The actual torque and flux are calculated simply using Equations (3) and (5), respectively. As a result, there is no requirement to design flux/torque estimators. The speed and angular position feedback signals are acquired using an encoder. Figure 2 depicts the block diagram of the proposed control approach.

Controllers Design

The speed, flux, and the current controllers are designed using the PI control method. Equation (8) provides the transfer function of the PI controller.

$$G_{PI} = K_p + \frac{K_i}{s} \tag{8}$$

K_p and K_i are the proportional and the integral gins, respectively. To find the gains of the PI controllers, the Ziegler–Nichols (ZN) method is used for tuning them [39,40]. A flowchart for the ZN method is presented in Figure 3.

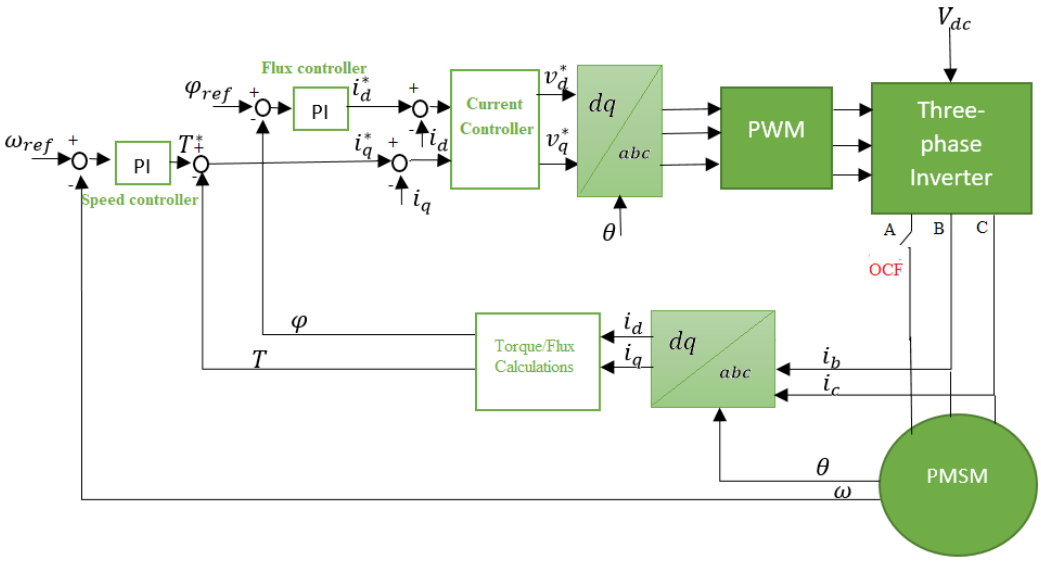

Figure 2. Scheme diagram illustrating OCF of PMSM with an independent speed and flux control.

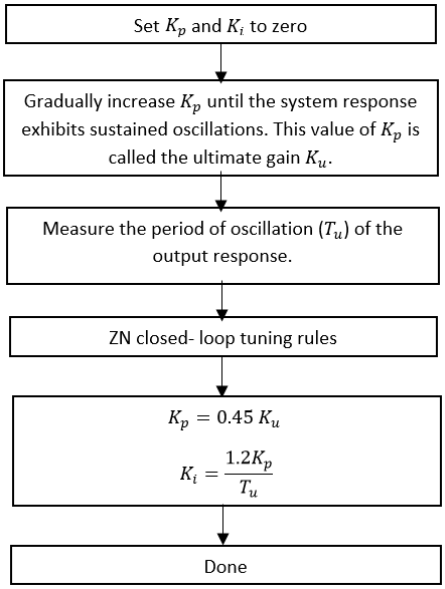

Figure 3. Ziegler–Nichols method procedure.

The error signal of the speed response and the flux response based on the ZN method are shown in Figure 4.

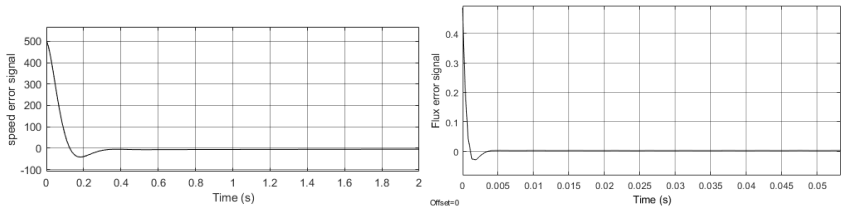

(**a**) (**b**)

Figure 4. (**a**) Speed error signal (**b**) Flux error signal.

4. Simulation Results

The performance of the PMSM was evaluated under the open-circuit fault condition using independent controllers for speed and flux. The evaluation was conducted through

modeling and testing in Matlab/Simulink. The Simulink model can be seen in Figure 5, while the parameters of the PMSM are listed in Table 1.

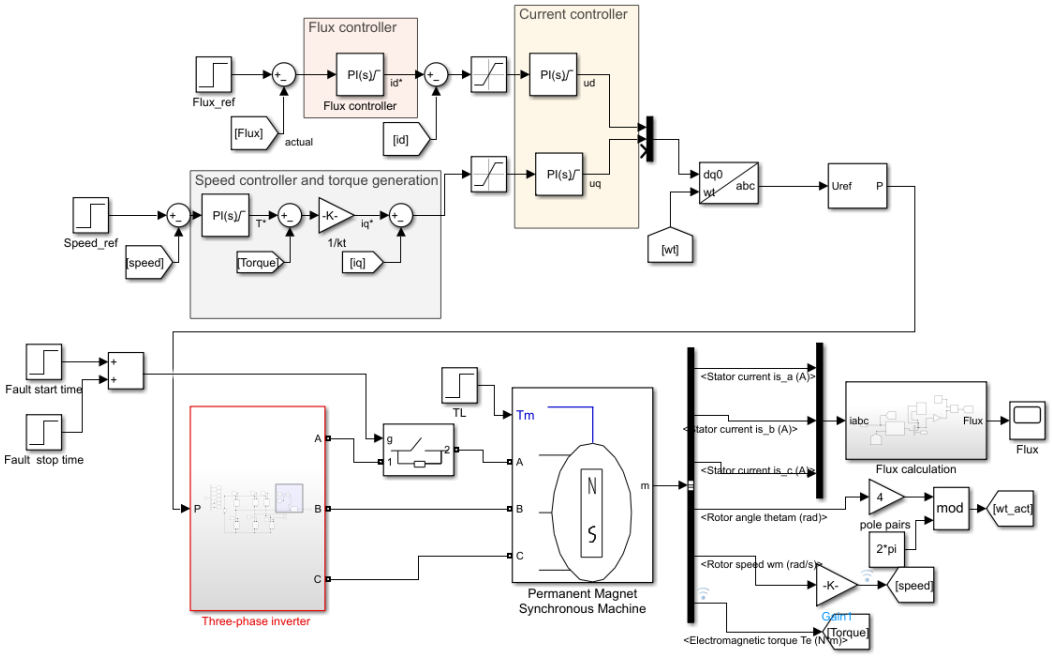

Figure 5. Matlab/Simulink model.

Table 1. Machine parameters.

Parameter	Value
Rated power	200 W
Rated voltage	42 V
Max speed	3000 RPM
Voltage constant	9.5 V/Krpm
Resistance (L-L)	0.4 Ohms
Inductance (L-L)	540 µH
Pole-pairs number	4
Magnetic flux linkage	0.01309 Wb

The motor's performance is showcased in various operational phases, including pre-fault, open-circuit fault, and post-fault. Specifically, the open-circuit fault operation demonstrates the PMSM's performance through three distinct scenarios: speed change, flux change, and load change.

The operation of the motor, along with the reference speed, reference flux, and load torque, are provided as shown in Equations (9)–(12).

$$\text{Motor operation} = \begin{cases} \text{Pre-fault operation}, & 0 < t < 1 \text{ s} \\ \text{OCF operation}, & 1 < t < 3.5 \text{ s} \\ \text{Post-fault operation}, & 3.5 < t < 5 \text{ s} \end{cases} \tag{9}$$

$$Speed_{ref} = \begin{cases} 150 \text{ rpm}, & 0 < t < 1.5 \text{ s} \\ 500 \text{ rpm}, & 1.5 < t < 5 \text{ s} \end{cases} \tag{10}$$

$$flux_{ref} = \begin{cases} 0.014 \text{ Wb}, & 0 < t < 2 \text{ s} \\ 0.016 \text{ Wb}, & 2 < t < 5 \text{ s} \end{cases} \tag{11}$$

$$T_L = \begin{cases} 0.1\ \text{N·m}, & 0 < t < 2.5\ \text{s} \\ 0.2\ \text{N·m}, & 2.5 < t < 5\ \text{s} \end{cases} \tag{12}$$

The motor operates in pre-fault with a 150 rpm reference speed, 0.014 Wb reference flux, and 0.1 N·m load torque. An open-circuit fault was observed on phase A at $t = 1$ s and resolved at $t = 3.5$ s. During the fault period, the speed was modified to 500 rpm at $t = 1.5$ s, the flux was adjusted to 0.016 Wb at $t = 2$ s, and the load was altered to 0.2 N·m at $t = 2.5$ s.

While the currents in phases B and C became larger and more distorted during the OCF operation, the current in phase A decreased to zero. As the flux is calculated based on the stator currents i_{abc}, the distortion in the currents during OCF leads to fluctuations in the flux response as well. Additionally, there is a slight reduction in the motor speed. Further, the OCF causes ripples in the speed and torque responses. The current response is stable under the OCF operation and during the three scenarios. After clearing the fault at $t = 3$ s, the current has a high transient response. However, it takes the motor 1 second to reach a steady state.

The transient response of the PMSM during the three operations exhibits the stator current performance depicted in Figure 6. Figure 7 as depicts the PMSM's speed response during the three operations, including the transient response. The speed controller consistently tracks the desired value throughout the operation, effectively adjusting to changes in speed, flux, and load torque. Despite the occurrence of small speed response fluctuations caused by the OCF, the motor consistently delivers satisfactory performance. As a result, this control method demonstrates robustness in the face of flux and load torque variations during the OCF, ensuring reliable operation. The current limits and machine size plays an important role in the flux control. In other words, there is certain boundaries for the flux reference so that it cannot proceed. However, for larger machines with higher ratings, these boundaries and flux control ranges can be larger and more flexible.

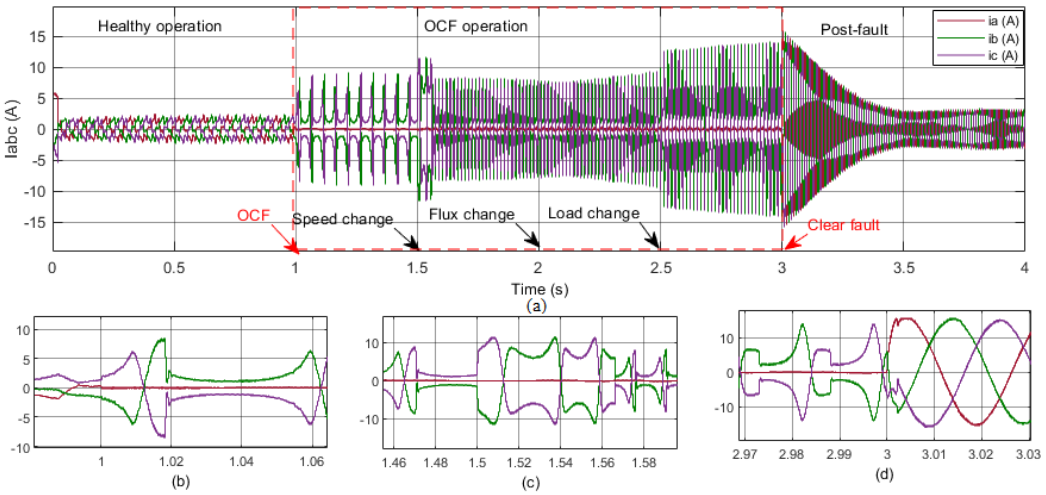

Figure 6. Stator currents of the PMSM during pre-fault, OCF, and post-fault operation: (**a**) Overall, (**b**) Transient during OCF, (**c**) Transient during speed change, and (**d**) Transient at post-fault operation.

Figure 8 illustrates the torque response throughout various operations and under different conditions, including speed, flux, and load torque variations. The presence of an open-circuit fault introduces slight fluctuations in the torque waveform. Even during the load change scenario, where the load torque is adjusted to 0.2 N·m, the motor exhibits a desirable response, even under open-circuit fault operation, demonstrating its resilience and performance.

The flux response of the PMSM under the three operations and with speed, flux, and load torque change is presented in Figure 9. As depicted in the figure, when $t = 1.5$ s,

the steady-state flux value remains unaffected by the speed variation. At $t = 2.5$ s, the load is changed, causing changes in the stator currents as well as in the flux response. At post-fault operation, the flux controller needs 1 s to regulate the flux and reach steady-state performance.

The responses of the dq-axis reference currents (I_d and I_q) are presented in Figures 10 and 11, respectively. I_d response follows the flux response based on Equation (3), while the I_q response follows the torque response based on Equation (6).

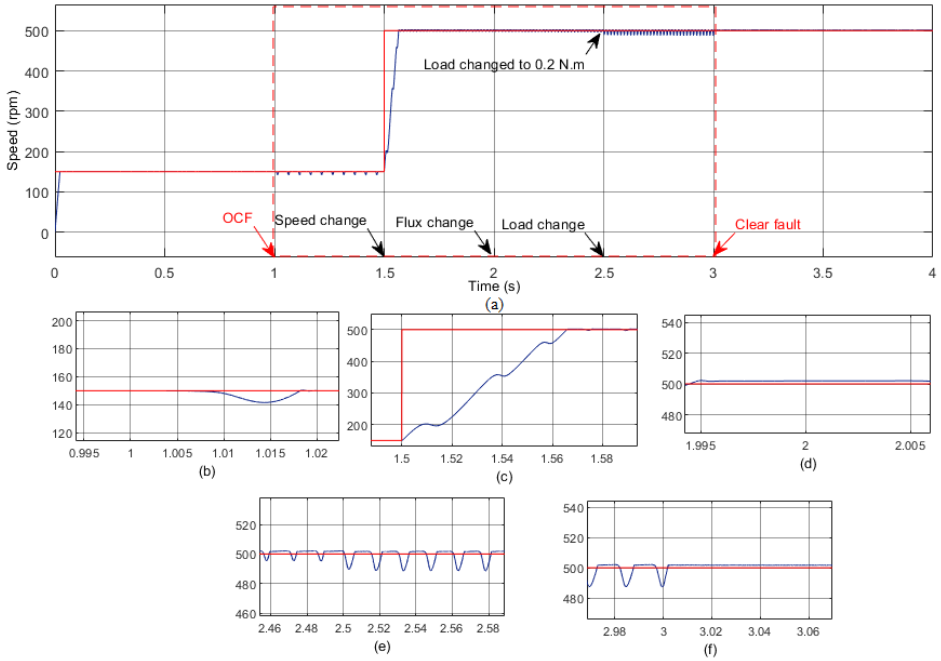

Figure 7. Speed response during the three operations: (**a**) Overall, (**b**) Transient at OCF, (**c**) Transient at speed change, (**d**) Transient at flux change, (**e**) Transient at load change, and (**f**) Transient at post-fault operation.

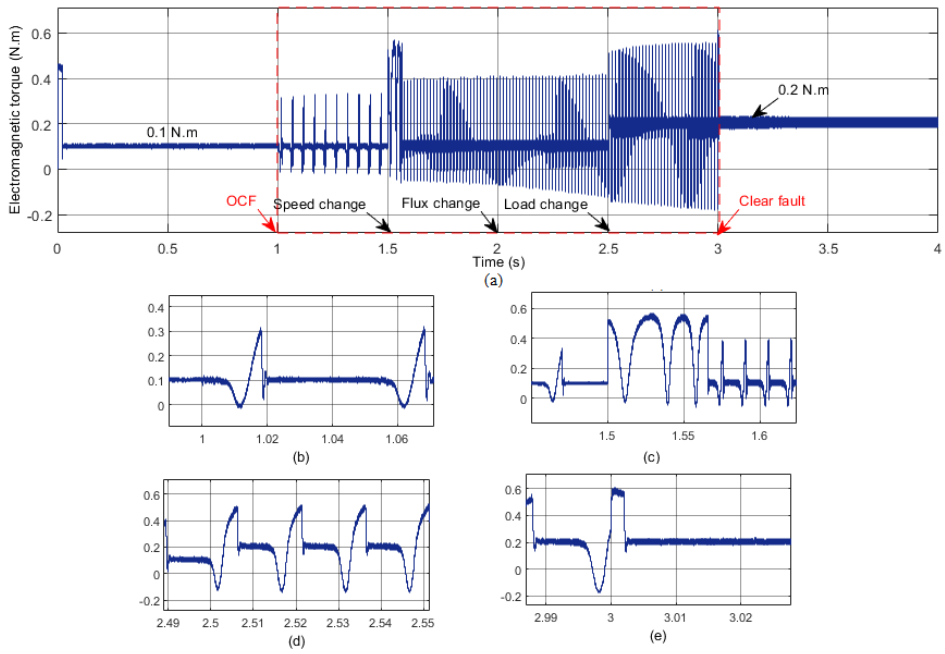

Figure 8. Electromagnetic Torque of PMSM under pre-fault, OCF, and post-fault operation: (**a**) Overall, (**b**) Transient at OCF, (**c**) Transient during speed change, (**d**) Transient during load torque change, and (**e**) Transient at post-fault operation.

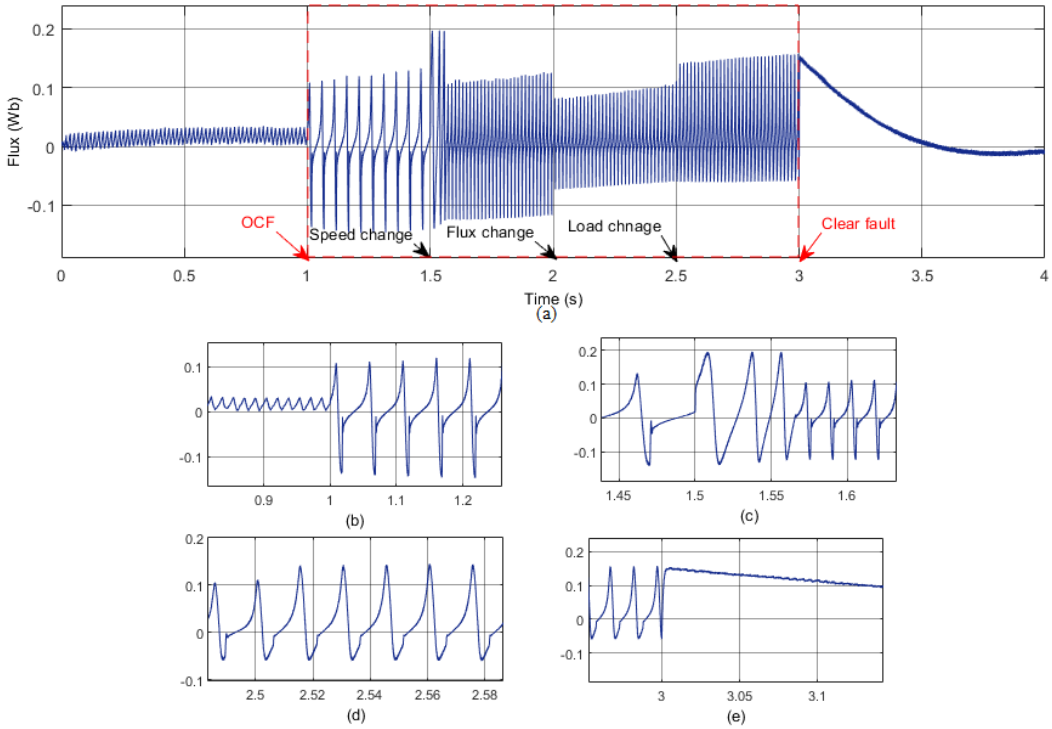

Figure 9. Flux response during the three operations: (**a**) Overall, (**b**) Transient at OCF, (**c**) Transient during speed change, (**d**) Transient at load torque change, and (**e**) Transient at post-fault operation.

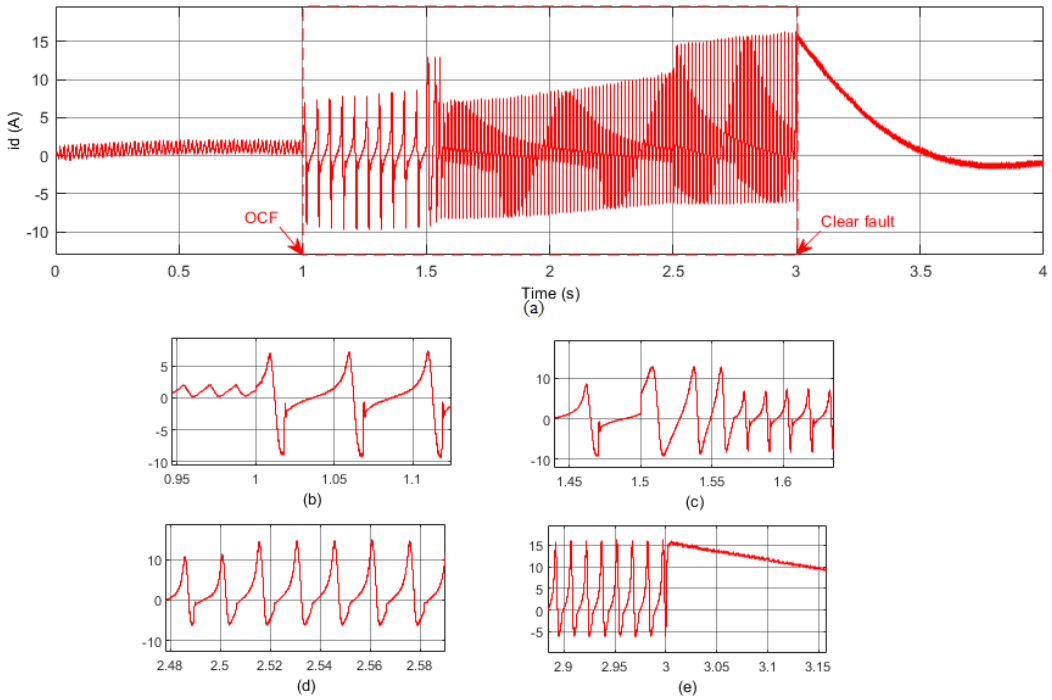

Figure 10. I_d response under pre-fault, OCF, and post-fault operation: (**a**) Overall, (**b**) Transient at OCF, (**c**) Transient during speed change, (**d**) Transient during load torque change, and (**e**) Transient at post-fault operation.

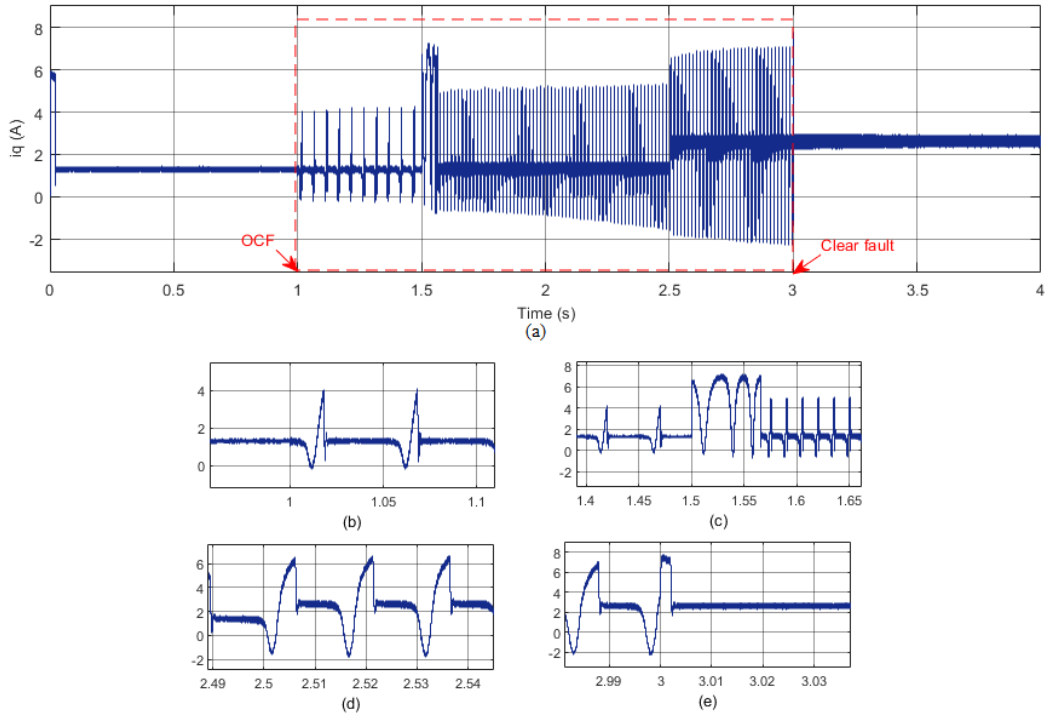

Figure 11. I_q response under pre-fault, OCF, and post-fault operation: (**a**) Overall, (**b**) Transient at OCF, (**c**) Transient during speed change, (**d**) Transient during load torque change, and (**e**) Transient at post-fault operation.

5. Hardware Experimental Results

In the experimental setup, a three-phase PMSM was linked to a three-phase inverter. The inverter board was supplied with 42 V. The dSPACE DS1104 was employed to implement the control algorithms as well as control the operation of the PMSM. The DC generator was connected to the PMSM as a load. The motor's parameters are listed in Table 1. Decoupled controllers were employed to regulate the speed and flux independently. The gains of the speed controller are ($K_P = 0.55372$, $K_i = 0.156321$) and those of the flux controller are ($K_P = 0.452$, $K_i = 10.7901$). Two PI current controllers handled the dq-currents. The d-axis reference current was generated through the flux controller. The gains of the current controllers are ($K_P = 0.0103$, $K_i = 2.2729$).The experimental configuration is shown in Figure 12.

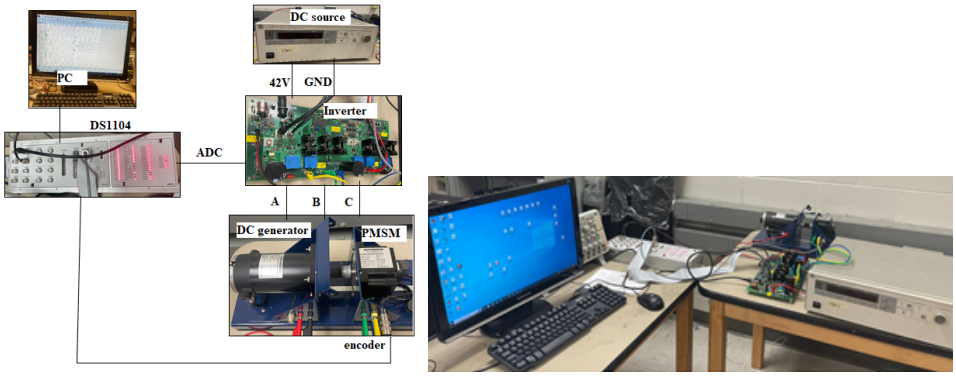

Figure 12. Hardware experimental platform.

The motor operated in the pre-fault condition with a target speed of 350 rpm, a load torque set-point of 0.1 N·m, and a desired flux level of 14 mwb, ensuring no similarity with other conditions. Then, the OCF occurred by disconnecting phase A at $t = 3.5$ s . To prove the efficacy of the control method under OCF operation, the motor was tested through flux

change, load torque change, and speed change. The flux was changed to 16 mWb at $t = 7$ s. Subsequently, the load torque was augmented to 0.3 N·m at $t = 10$ s. Following that, the speed was increased to 500 rpm at $t = 14.15$ s. Phase A was subsequently reconnected to the motor, and the fault was resolved at $t = 19$ s.

The stator current responses of the PMSM during various operations and scenarios are illustrated in Figure 13. During an OCF in phase A, the current in phase A drops to zero, while the currents in phases B and C show distortion. Figure13a–d represent the transient responses during OCF, flux change, speed change, and post-fault operation, respectively. After clearing the fault, the current response of the PMSM reaches steady-state performance in 3 s, which means the motor needs some time to perform as in pre-fault operation.

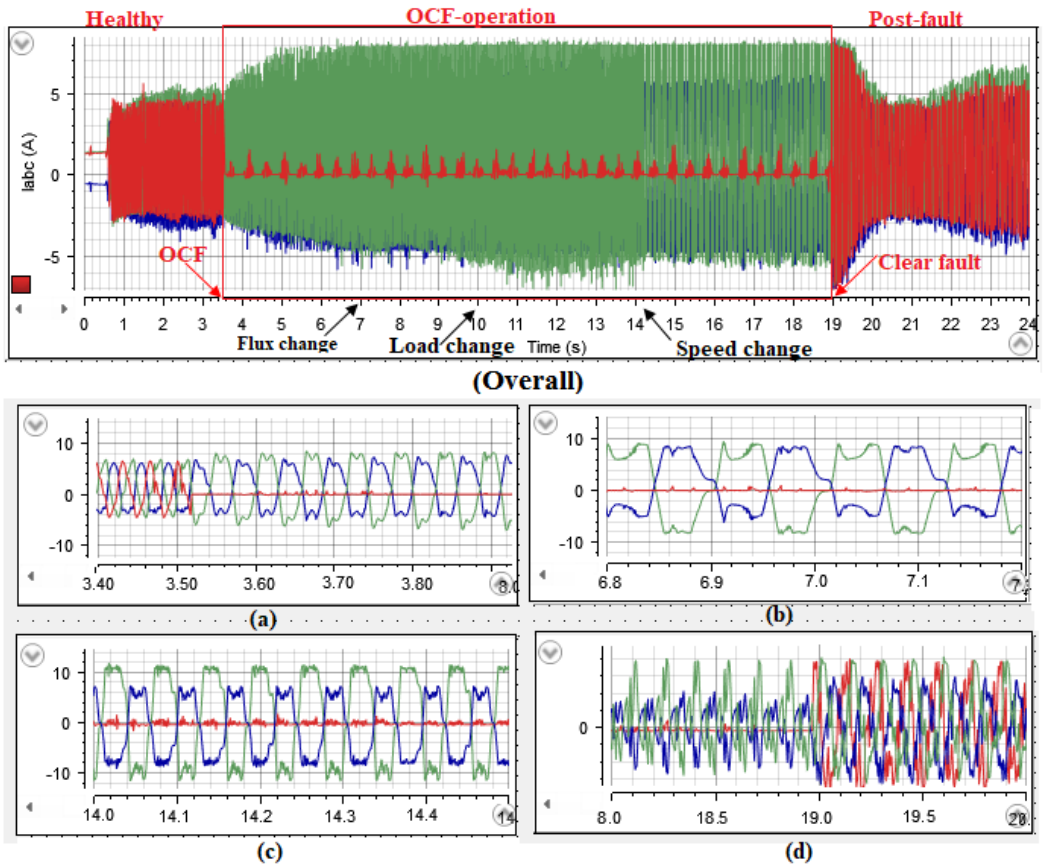

Figure 13. (**Overall**) PMSM stator currents during pre-fault, OCF, and post-fault operations: (**a**) Transient at OCF, (**b**) Transient at flux change, (**c**) Transient at speed change, and (**d**) Transient at post-fault operation.

The speed performance during the three motor operations and during the flux change, load torque change, and speed change are as shown in Figure 14. In addition, the transient responses at fault, flux change, speed change, and after fault are presented in Figure14a–d, respectively. The speed controller effectively follows the desired reference value during open-circuit fault situations across all three scenarios. Although minor ripples are observed in the speed response during open-circuit fault, they do not impact the overall motor performance. The motor still spins at its speed smoothly and with stability. Once the fault is cleared, the speed controller rapidly stabilizes, and when the load torque is elevated in the presence of the open-circuit fault, the motor speed decreases.

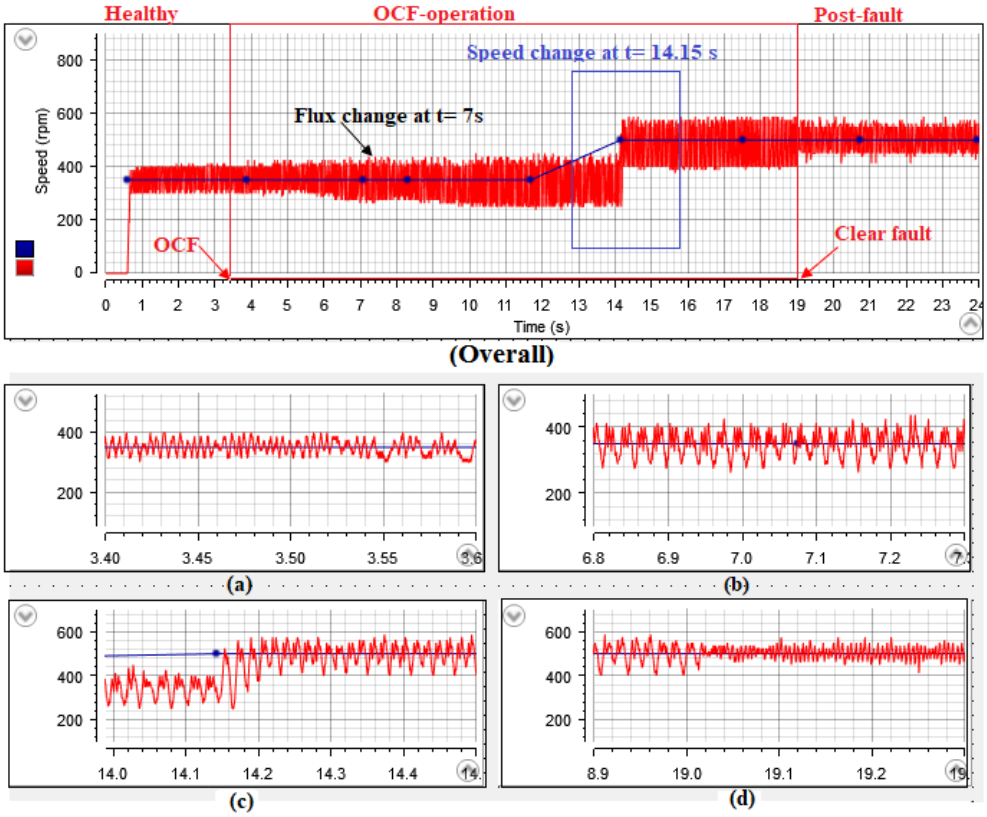

Figure 14. (**Overall**) Speed performance during pre-fault, OCF, and post-fault operations: (**a**) Transient at OCF, (**b**) Transient at flux change, (**c**) Transient at speed change, and (**d**) Transient at post-fault operation.

Figure 15 illustrates the torque response of the PMSM during the transient period. Additionally, Figure 16 showcases the flux performance throughout the pre-fault, OCF, and post-fault operations, encompassing scenarios involving flux change, load change, and speed change. The stability of the flux during the OCF operation and its independence in controlling the speed and load can be observed. Furthermore, during the post-fault operation, the flux gradually returns to its pre-fault state within a time frame of 3 s.

The response of I_d and I_q and their transients during the OCF, flux change, speed change, and post-fault operation are as shown in Figure 17 and Figure 18, respectively. I_d is related to the flux. Hence, a similar response is expected. The generation of I_q is dependent on the torque, thus leading to a similar response.

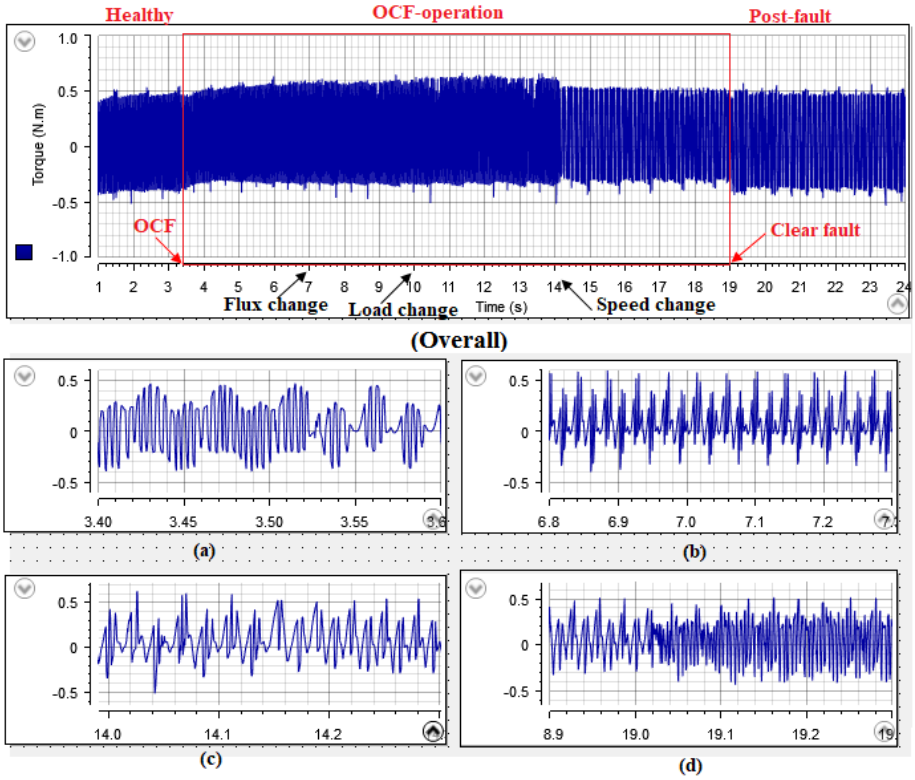

Figure 15. (**Overall**) Torque performance during pre-fault, OCF, and post-fault operations: (**a**) Transient at OCF, (**b**) Transient at flux change, (**c**) Transient at speed change, and (**d**) Transient at post-fault operation.

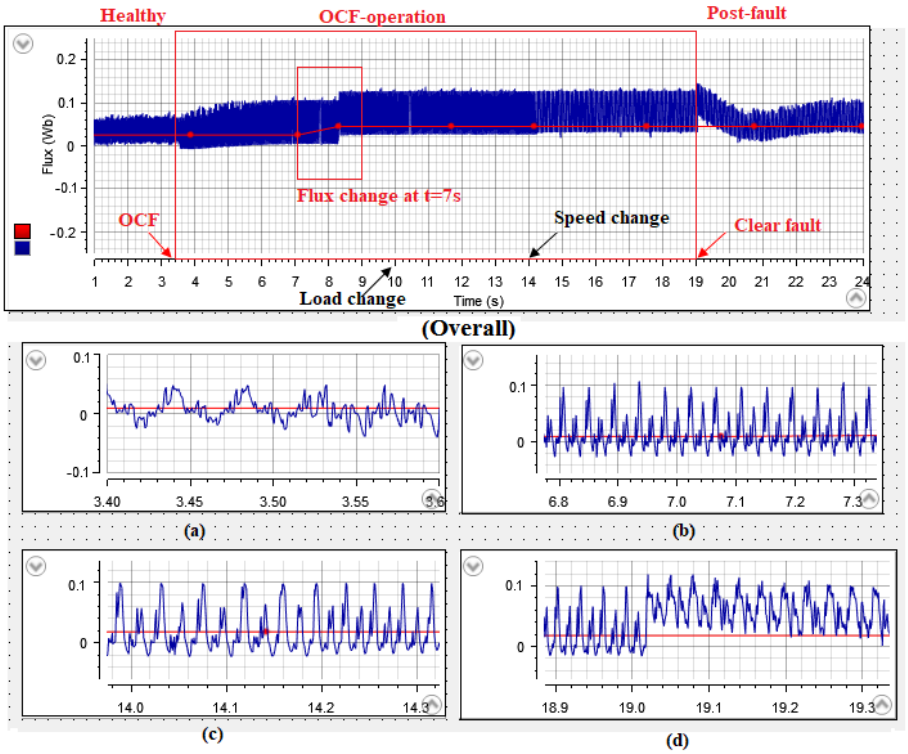

Figure 16. (**Overall**) Flux performance during pre-fault, OCF, and post-fault operations: (**a**) Transient at OCF, (**b**) Transient at flux change, (**c**) Transient at speed change, and (**d**) Transient at post-fault operation.

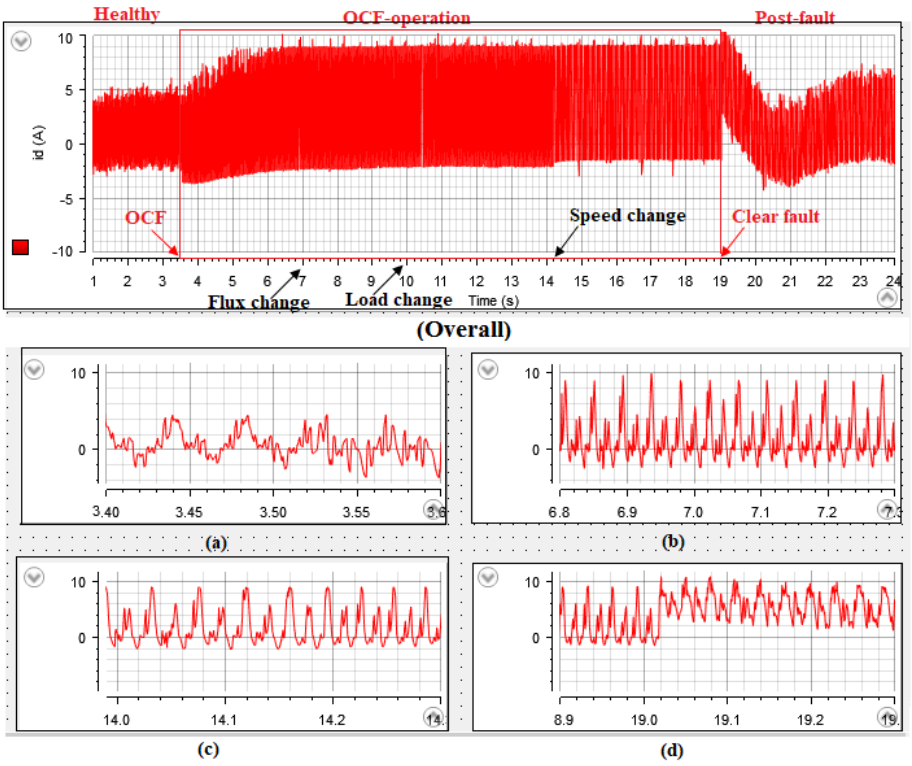

Figure 17. (**Overall**) I_d performance during pre-fault, OCF, and post-fault operations: (**a**) Transient at OCF, (**b**) Transient at flux change, (**c**) Transient at speed change, and (**d**) Transient at post-fault operation.

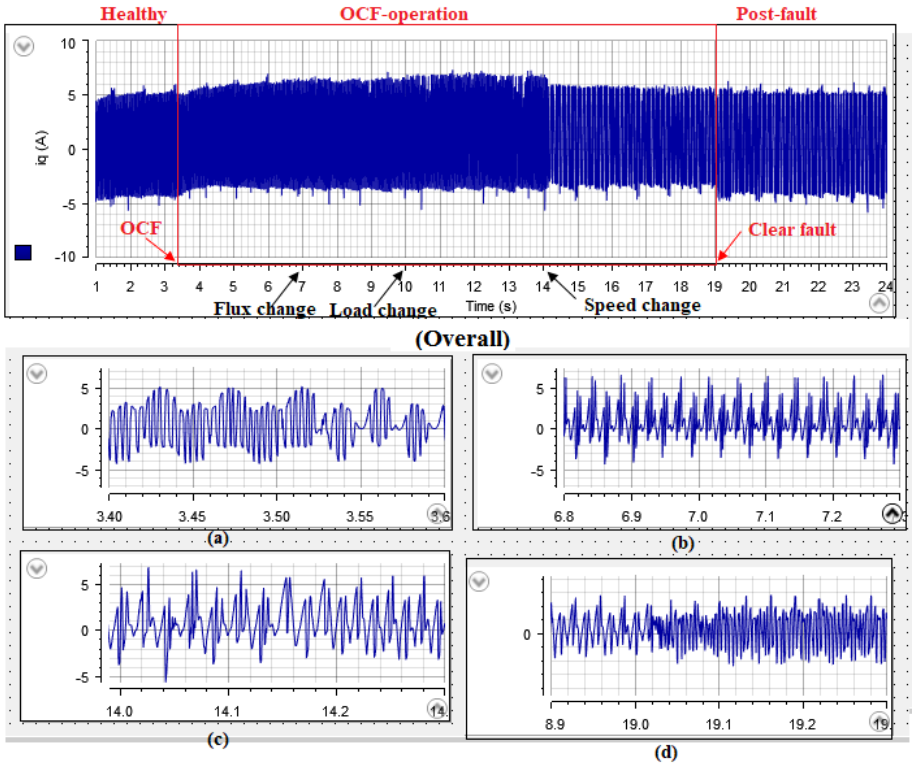

Figure 18. (**Overall**) I_q performance during pre-fault, OCF, and post-fault operations: (**a**) Transient at OCF, (**b**) Transient at flux change, (**c**) Transient at speed change, and (**d**) Transient at post-fault operation.

6. Conclusions

This article introduces the operation of a three-phase PMSM under OCF conditions using independent control of speed and flux. The motor's performance is analyzed in pre-fault, open-circuit fault, and post-fault scenarios. Specifically, the focus is on the performance during open-circuit fault operation, considering variations in flux, load torque, and speed. The transient response during these different operations and scenarios was also investigated. There is a limitation to the reference flux selection. However, for larger machines with higher current ratings, these boundaries and flux control range can be larger and more flexible.

The simulation and experimental findings demonstrate the control method's effectiveness in sustaining uninterrupted motor operation during the occurrence of open-circuit faults. Thus, the motor still operates with stable performance. In addition, the results show the robustness of the control method against the open-circuit fault and within the speed, flux, and load torque changes.

As a future work, an adaptive PIR controller will be proposed to mitigate the torque ripples under open-circuit fault operation

Author Contributions: Conceptualization, H.G., M.A. and R.M.N.; methodology, H.G.; software, H.G.; validation, H.G., M.A. and R.M.N.; formal analysis, H.G; investigation,H.G., M.A. and R.M.N.; supervision, R.M.N. All authors have read and agreed to the published version of the manuscript.

Funding: This research received no external funding.

Data Availability Statement: Data are contained within the article.

Conflicts of Interest: The authors declare no conflicts of interest.

Nomenclature

The following nomenclature are used in this manuscript:

Rs	PMSM phase resistance
i_{abc}	motor currents phases a , b, c
i_d	motor current d-axis component
i_q	motor current q-axis component
k_e	voltage constant of PMSM
k_i	integral component gain
k_p	proportional component gain
k_t	torque constant
L_d	PMSM d-axis inductance
L_q	PMSM q-axis inductance
p	number of pole pairs
T_e	the electromagnetic torque
t	time
V_d	the stator voltage of PMSM in d-axis
V_q	the stator voltage of PMSM in q-axis
ψ_m	permanent magnetic flux linkage
ψ_d	flux linkage of the stator in d-axis
ψ_q	flux linkage of the stator in q-axis
θ_r	rotor angle position
ω	the fundamental angular frequency
ω_r	electrical rotor speed

References

1. Ghanayem, H.; Alathamneh, M.; Nelms, R.M. A comparative study of PMSM torque control using proportional-integral and proportional-resonant controllers. *SoutheastCon* **2022**, *2022*, 453–458.
2. Dwivedi, S.K.; Laursen, M.; Hansen, S. Voltage vector based control for PMSM in industry applications. In Proceedings of the IEEE International Symposium on Industrial Electronics, Bari, Italy, 4–7 July 2010; pp. 3845–3850.

3. Abassi, M.; Khlaief, A.; Saadaoui, O.; Chaari, A.; Boussak, M. Performance analysis of FOC and DTC for PMSM drives using SVPWM technique. In Proceedings of the 16th International Conference on Sciences and Techniques of Automatic Control and Computer Engineering (STA), Monastir, Tunisia, 21–23 December 2015; pp. 228–233.
4. Korkmaz, F.; Topaloğlu, I.; Çakir, M.F.; Gürbüz, R. Comparative performance evaluation of FOC and DTC controlled PMSM drives. In Proceedings of the 4th International Conference on Power Engineering, Energy and Electrical Drives, Istanbul, Turkey, 13–17 May 2013; pp. 705–708.
5. Gupta, N.P.; Gupta, P. Performance analysis of direct torque control of PMSM drive using SVPWM—Inverter. In Proceedings of the IEEE 5th India International Conference on Power Electronics (IICPE), Delhi, India, 6–8 December 2012; pp. 1–6.
6. Tang, M.; Zhuang, S. On Speed Control of a Permanent Magnet Synchronous Motor with Current Predictive Compensation. *Energies* **2019**, *12*, 65. [CrossRef]
7. Codreş, B.; Găiceanu, M.; Şolea, R.; Eni, C. Model predictive speed control of Permanent Magnet Synchronous Motor. In Proceedings of the International Conference on Optimization of Electrical and Electronic Equipment (OPTIM), Bran, Romania, 22–24 May 2014; pp. 477–482.
8. Nicola, C.-I.; Nicola, M.; Vintilă, A.; Sacerdoţianu, D. Identification and Sensorless Control of PMSM Using FOC Strategy and Implementation in Embedded System. In Proceedings of the 2019 International Conference on Electromechanical and Energy Systems (SIELMEN), Craiova, Romania, 9–11 October 2019; pp. 1–6.
9. Wang, Z.; Yang, J.; Ye, H.; Zhou, W. A review of Permanent Magnet Synchronous Motor Fault diagnosis. In Proceedings of the 2014 IEEE Conference and Expo Transportation Electrification Asia-Pacific (ITEC Asia-Pacific), Beijing, China, 31 August–3 September 2014.
10. Welchko, B.A.; Jahns, T.M.; Hiti, S. IPM synchronous machine drive response to a single-phase open circuit fault. *IEEE Trans. Power Electron.* **2002**, *17*, 764–771. [CrossRef]
11. Ghanayem, H.; Alathamneh, M.; Nelms, R.M. Three-phase PMSM vector control using decoupled flux and Speed Controller. *Energy Rep.* **2023**, *9*, 645–652. [CrossRef]
12. Solís, R.; Torres, L.; Pérez, P. Review of methods for diagnosing faults in the stators of BLDC Motors. *Processes* **2022**, *11*, 82. [CrossRef]
13. Morel, C.; Gueux, B.L.; Rivero, S.; Chahba, S. Currents analysis of a brushless motor with inverter faults—Part II: Diagnostic method for open-circuit fault isolation. *Actuators* **2023**, *12*, 230. [CrossRef]
14. Zhou, Y.; Yao, F.; Zhao, S. Torque superposition compensation fault-tolerant control for dual three-phase PMSM with an inverter single-leg open-circuit fault. *Energies* **2022**, *15*, 6053. [CrossRef]
15. Huang, W.; Du, J.; Hua, W.; Lu, W.; Bi, K.; Zhu, Y.; Fan, Q. Current-based open-circuit fault diagnosis for PMSM drives with model predictive control. *IEEE Trans. Power Electron.* **2021**, *36*, 10695–10704. [CrossRef]
16. Huang, W.; Du, J.; Hua, W.; Fan, Q. An open-circuit fault diagnosis method for PMSM drives using symmetrical and DC components. *Chin. J. Electr. Eng.* **2021**, *7*, 124–135. [CrossRef]
17. Canseven, H.T.; Unsal, A. Performance improvement of a five-phase PMSM drive under open circuit stator faults. In Proceedings of the 2021 5th International Symposium on Multidisciplinary Studies and Innovative Technologies (ISMSIT), Ankara, Turkey, 21–23 October 2021.
18. Huang, W.; Hua, W.; Fan, Q. Performance analysis and comparison of two fault-tolerant model predictive control methods for five-phase PMSM drives. *CES Trans. Electr. Mach. Syst.* **2021**, *5*, 311–320. [CrossRef]
19. Huang, W.; Hua, W.; Chen, F.; Hu, M.; Zhu, J. Model predictive torque control with SVM for five-phase PMSM under open-circuit fault condition. *IEEE Trans. Power Electron.* **2020**, *35*, 5531–5540. [CrossRef]
20. Liu, L.; Zhang, Q. Open-circuit fault-tolerant control of a six-phase asymmetric permanent magnet synchronous motor drive system. *Electronics* **2023**, *12*, 1131. [CrossRef]
21. Suti, A.; Di Rito, G. Diagnosis of Power Switch Faults in Three-Phase Permanent Magnet Synchronous Motors via Current-Signature Technique. *Actuators* **2024**, *13*, 25. [CrossRef]
22. Mohammadi, F.; Saif, M. A Multi-Stage Hybrid Open-Circuit Fault Diagnosis Approach for Three-Phase VSI-Fed PMSM Drive Systems. *IEEE Access* **2023**, *11*, 137328–137342. [CrossRef]
23. Wang, X.; Ren, S.; Xiao, D.; Meng, X.; Fang, G.; Wang, Z. Fault-Tolerant Control of Open-Circuit Faults in Standard PMSM Drives Considering Torque Ripple and Copper Loss. *IEEE Trans. Transp. Electrif.* **2023.** [CrossRef]
24. Wang, F.; Li, S.; Mei, X.; Xie, W.; Rodríguez, J.; Kennel, R.M. Model-based predictive direct control strategies for electrical drives: An experimental evaluation of PTC and PCC methods. *IEEE Trans. Ind. Inf.* **2015**, *11*, 671–681. [CrossRef]
25. Li, P.; Xu, X.; Yang, S.; Jiang, X. Open circuit fault diagnosis strategy of PMSM drive system based on grey prediction theory for Industrial Robot. *Energy Rep.* **2023**, *9*, 313–320. [CrossRef]
26. Ghanayem, H.; Alathamneh, M.; Nelms, R.M. Performance of a vector controlled PMSM drive based on proportional–resonance control under single-phase open circuit fault. *Energy Rep.* **2023**, *9*, 755–763. [CrossRef]
27. Ghanayem, H.; Alathamneh, M.; Nelms, R.M. Adaptive PIR Current Controllers for Torque Ripple Reduction of PMSM using Decoupled Speed and Flux Control. In Proceedings of the 2023 IEEE 14th Annual Ubiquitous Computing, Electronics & Mobile Communication Conference (UEMCON), New York, NY, USA, 2023; pp. 0440–0444. [CrossRef]
28. Wang, W.; Zhang, J.; Cheng, M. Common model predictive control for permanent-magnet synchronous machine drives considering single-phase open-circuit fault. *IEEE Trans. Power Electron.* **2017**, *32*, 5862–5872. [CrossRef]

29. Qiu, X.; Ji, J.; Zhou, D.; Zhao, W.; Chen, Y.; Huang, L. A modified flux observer for sensorless direct torque control of dual three-phase PMSM considering open-circuit fault. *IEEE Trans. Power Electron.* **2022**, *37*, 15356–15369. [CrossRef]
30. Scarcella, G.; Scelba, G.; Pulvirenti, M.; Lorenz, R.D. Fault-tolerant capability of deadbeat-direct torque and Flux Control for three-phase PMSM drives. *IEEE Trans. Ind. Appl.* **2017**, *53*, 5496–5508. [CrossRef]
31. Zhou, H.; Zhao, W.; Liu, G.; Cheng, R.; Xie, Y. Remedial field-oriented control of five-phase fault-tolerant permanent-magnet motor by using reduced-order transformation matrices. *IEEE Trans. Ind. Electron.* **2017**, *64*, 169–178. [CrossRef]
32. Chai, F.; Gao, L.; Yu, Y.; Liu, Y. Fault-tolerant control of modular permanent magnet synchronous motor under open-circuit faults. *IEEE Access* **2019**, *7*, 154008–154017. [CrossRef]
33. Dwari, S.; Parsa, L.; Lipo, T.A. Optimum control of a five-phase integrated modular permanent magnet motor under normal and open-circuit fault conditions. In Proceedings of the 2007 IEEE Power Electronics Specialists Conference, Orlando, FL, USA, 17–21 June 2007.
34. Zhou, H.; Zhou, C.; Tao, W.; Wang, J.; Liu, G. Virtual-stator-flux-based direct torque control of five-phase fault-tolerant permanent-magnet motor with open-circuit fault. *IEEE Trans. Power Electron.* **2020**, *35*, 5007–5017. [CrossRef]
35. Wang, B.; Feng, X.; Wang, R. Open-Circuit Fault Diagnosis for Permanent Magnet Synchronous Motor Drives Based on Voltage Residual Analysis. *Energies* **2023**, *16*, 5722. [CrossRef]
36. Rahman, A.; Dutta, R.; Chu, G.; Xiao, D.; Thippiripati, V.K.; Rahman, M.F. Open-Winding Permanent Magnet Synchronous Generator for Renewable Energy—A Review. *Energies* **2023**, *16*, 5268. [CrossRef]
37. Geng, Q.; Li, Z.; Wang, H.; Zhang, G.; Zhou, Z. Natural Fault-Tolerant Control With Minimum Copper Loss in Full Torque Operation Range for Dual Three-Phase PMSM Under Open-Circuit Fault. *IEEE Trans. Power Electron.* **2024**, *39*, 1279–1291. [CrossRef]
38. Campos-Delgado, D.U.; Pecina-Sánchez, J.A.; Espinoza-Trejo, D.R.; Arce-Santana, E.R. Diagnosis of open-switch faults in variable speed drives by stator current analysis and pattern recognition. *IET Electr. Power Appl.* **2013**, *7*, 509–522. [CrossRef]
39. Alathamneh, M.; Ghanayem, H.; Nelms, R.M. Power Control of a Three-phase Grid-connected Inverter using a PI Controller under Unbalanced Conditions. In Proceedings of the SoutheastCon 2022, Mobile, AL, USA, 26 March–3 April 2022; pp. 447–452
40. Ziegler, J.G.; Nichols, N.B. Optimum Settings for Automatic Controllers. *J. Dyn. Syst. Meas. Control* **1993**, *115*, 220–222. [CrossRef]